On the Minimal Average Distortion of Parameter Optimized Quantizers

Jun Guo, Philipp Walk, and Hamid Jafarkhani
Center for Pervasive Communications and Computing, Electrical Engineering Hall
University of California, Irvine, CA 92697-2625
{guoj4,pwalk,hamidj}@uci.edu

Abstract

In many quantization problems, the distortion function is given by the Euclidean norm to measure the distance of a source sample to any given reproduction point of the quantizer. We will in this work regard distortion functions, which are additively and multiplicatively weighted for each reproduction point resulting in a heterogeneous quantization problem, as used for example in deployment problems of sensor networks. Whereas, in such problems, the average distortion is minimized for given weights (parameters), we will optimize the quantization problem over all weights, i.e., we tune or control the distortion functions in our favour. For a uniform source distribution in one-dimension we derived the unique minimizer, given as the uniform scalar quantizer with an optimal common weight. By numerical simulations, we demonstrate that this result extends to two-dimensions where asymptotically the parameter optimized quantizer is the hexagonal lattice with common weights. As an application we will determine the optimal deployment of unmanned aerial vehicles (UAV) to provide a wireless communication to ground terminals under a minimal communication power cost. Here, the optimal weights refer to the optimal flight heights of the UAVs.

1 Introduction

For a convex set $\Omega \in \mathbb{R}^d$ in $d = 1, 2$ dimensions a quantizer is given by N reproduction or quantization points $\mathbf{Q} = \{\mathbf{q}_1, \ldots, \mathbf{q}_N\} \subset \Omega$ associated with N quantization regions $\mathcal{R} = \{\mathcal{R}_1, \ldots, \mathcal{R}_N\} \subset \Omega$, defining a partition of Ω. To measure the distortion of a given quantizer, the Euclidean distance between the source samples and reproduction points is commonly used as the distortion function. We will study in this work quantizers with parameter depending distortion functions which minimize the average distortion over Ω for a given continuous source sample distribution $\lambda : \Omega \to [0, 1]$, as investigated for example in [1]–[3]. Contrary to a fixed parameter selection [1], we will assign to each quantization point $\mathbf{q}_n$ variable parameters to control the distortion function of the nth quantization point. Such a controllable distortion function widens the scope of quantization theory and allows to apply quantization techniques to many parameter dependent network and locational problems. In this work, we will consider for the distortion function of $\mathbf{q}_n$ the Euclidean square-distance, which is multiplicative weighted by some $a_n > 0$ and additively weighted by some $b_n > 0$. Furthermore, we exponentially weight all distortion functions by some fixed exponent $\gamma \geq 1$. To minimize the average distortion, the optimal quantization regions are known to be generalized Voronoi (Möbius) regions, which can be non-convex and disconnected sets [4]. In many applications, as in sensor or vehicle deployments, the optimal weights and parameters are usually unknown, but adjustable, and one wishes therefore to optimize the deployment over all admissible parameter values, see for example [3]. We will

in this work characterize such *parameter optimized quantizers* over one-dimensional convex target regions, i.e., over closed intervals. As a motivation we will demonstrate such a parameter driven quantizer for an unmanned aerial vehicle (UAV) deployment to provide energy efficiently a communication to ground terminals in a given target region. Here the parameters refer to the UAVs flight heights. Due to page limitations, all proofs are presented in [5].

Notation By $[N] = \{1, 2, \ldots, N\}$ we denote the first N natural numbers of $\mathbb{N}$. We will write real numbers in $\mathbb{R}$ by small letters and row vectors by bold letters. The Euclidean norm of $\mathbf{x}$ is given by $\|\mathbf{x}\| = \sqrt{\sum_n x_n^2}$. The open ball in $\mathbb{R}^d$ centered at $\mathbf{c} \in \mathbb{R}^d$ with radius $r \geq 0$ is denoted by $\mathcal{B}(\mathbf{c}, r) = \{\boldsymbol{\omega} \mid \|\boldsymbol{\omega} - \mathbf{c}\|^2 \leq r\}$. We denote by $\mathcal{V}^c$ the complement of the set $\mathcal{V} \subset \mathbb{R}^d$. The positive real numbers are denoted by $\mathbb{R}_+ := \{a \in \mathbb{R} \mid a > 0\}$. Moreover, for two points $\mathbf{a}, \mathbf{b} \in \mathbb{R}^d$, we denote the generated half space between them, which contains $\mathbf{a} \in \mathbb{R}^d$ as $\mathcal{H}(\mathbf{a}, \mathbf{b})$.

2 System model

To motivate the concept of parameter optimized quantizers we will investigate the deployment of N UAVs positioned at $\mathbf{P} = \{\mathbf{p}_1, \ldots, \mathbf{p}_N\} \subset (\Omega \times \mathbb{R}_+)^N$ to provide a wireless communication link to ground terminals in a given target region $\Omega \subset \mathbb{R}^d$. Here, the nth UAVs position $\mathbf{p}_n = (\mathbf{q}_n, h_n)$ is given by its ground position $\mathbf{q}_n = (x_n, y_n) \in \Omega$, representing the quantization point, and its flight height h_n, representing its additional parameter. The optimal UAV deployment (parameter quantizer) is then defined by the minimal average communication power (distortion) to serve ground terminals distributed by λ in Ω with a minimal given data rate R_b. Hereby, each ground terminal will select the UAV which requires the smallest communication power, resulting in so called generalized Voronoi (quantization) regions of Ω, as used in [1]–[3], [6]–[10].

In the recent decade, UAVs with directional antennas have been widely studied in the literature [11]–[16], to increase the efficiency of wireless links. However, in [11]–[16], the antenna gain was approximated by a constant within a 3dB beamwidth and set to zero outside. This ignores the strong angle dependent gain of directional antennas, notably for low-altitude UAVs. To obtain a more realistic model we will consider here an antenna gain, which depends on the actual radiation angle $\theta_n \in [0, \frac{\pi}{2}]$ from the nth UAV at $\mathbf{p}_n$ to a GT at $\boldsymbol{\omega}$, see Figure 1. To capture the power falloff versus the line-of-sight distance d along with the random attenuation about the path loss from shadowing, we adopt the propagation model [17, (2.51)] as:

$$PL_{dB} = 10 \log_{10} K - 10\alpha \log_{10}(d/d_0) - \psi_{dB}, \tag{1}$$

where K is a unitless constant depending on the antenna characteristics, d_0 is a reference distance, $\alpha \geq 1$ is the terrestrial path loss exponent, and ψ_{dB} is a Gaussian random variable following $\mathcal{N}\left(0, \sigma^2_{\psi_{dB}}\right)$. This air-to-ground or terrestrial path loss model is widely used for UAV basestation path-loss models [18]. Practical values are

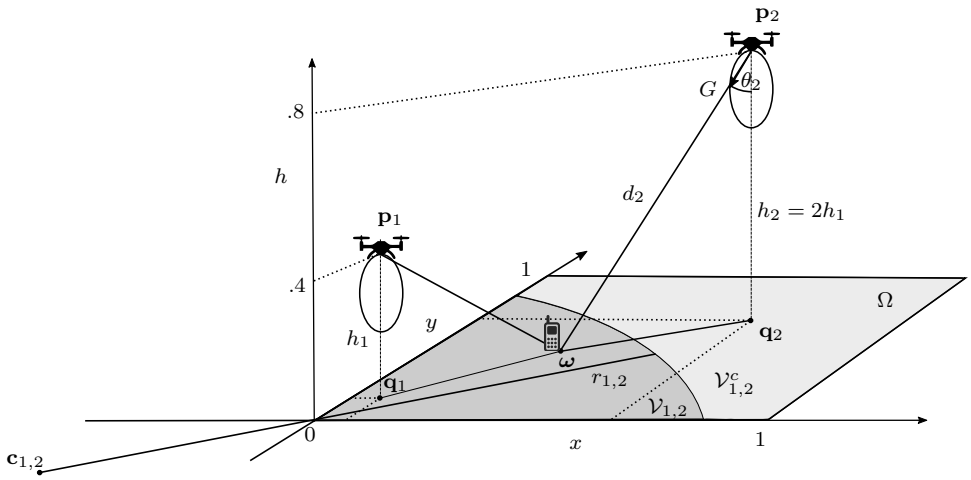

Figure 1: UAV deployment with directed antenna beam and associated GT cells for $\alpha = 2$ and $N = 2$ for a uniform GT distribution.

between 2 and 6 and depend on the Euclidean distance d of GT $\boldsymbol{\omega}$ and UAV $\mathbf{p}_n$

$$d_n(\boldsymbol{\omega}) = d(\mathbf{p}_n, (\boldsymbol{\omega}, 0)) = \sqrt{\|\mathbf{q}_n - \boldsymbol{\omega}\|^2 + h_n^2} = \sqrt{(x_n - x)^2 + (y_n - y)^2 + h_n^2} \tag{2}$$

and the shadowing due to low altitude. For common practical measurements see for example [19]. Typically maximal heights for UAVs are < 1000m, due to flight zone restrictions of aircrafts. Hence, the received power at UAV n can be represented as $P_{RX} = P_{TX} G_{TX} G_{RX} PL = P_{TX} G_{TX} G_{RX} K d_0^{\alpha} d_n^{-\alpha}(\boldsymbol{\omega}) 10^{-\frac{\psi_{dB}}{10}}$, where G_{TX} and G_{RX} are the antenna gains of the transmitter and the receiver, respectively. Here, we assume perfect omnidirectional transmitter (GT) antennas with an isotropic gain and directional receiver (UAV) antennas. The angle dependent antenna gains are

$$G_{\mathrm{GT}} > 0 \quad , \quad G_{\mathrm{UAV}} = \cos(\theta_n) = h_n / d_n(\boldsymbol{\omega}), \tag{3}$$

see [20, pp.52]. The combined antenna intensity is then proportional to $G = G_{\mathrm{UAV}} G_{\mathrm{GT}} K$, see Figure 1. Accordingly, the received power can be rewritten as

$$P_{RX} = P_{TX} h_n G_{\mathrm{GT}} K d_0^{\alpha} d_n^{-\alpha-1}(\boldsymbol{\omega}) 10^{-\frac{\psi_{dB}}{10}}. \tag{4}$$

To achieve the reliable communication between GT and UAV with bit-rate at least R_b, we get for a channel bandwidth B and noise power density N_0 by the Shannon capacity $B \log_2\left(1 + \frac{P_{RX}}{BN_0}\right) \geq R_b$ The minimum transmission power to UAV $\mathbf{p}_n$ is then given by $P_{TX} = \left(2^{\frac{R_b}{B}} - 1\right) B N_0 d(\mathbf{p}_n, (\boldsymbol{\omega}, 0))^{\alpha+1} 10^{\frac{\psi_{dB}}{10}} (h_n G_{\mathrm{GT}} K d_0^{\alpha})^{-1}$. The expectation

$$\begin{aligned} D(\boldsymbol{\omega}, \mathbf{q}_n, h_n) := \mathbb{E}[P_{TX}] &= \frac{(2^{\frac{R_b}{B}} - 1) N_0}{h_n G_{\mathrm{GT}} K d_0^{\alpha}} \frac{d_n^{\alpha+1}(\boldsymbol{\omega})}{\sqrt{2\pi}\sigma_{\psi_{dB}}} \int_{\mathbb{R}} \exp\left(-\frac{\psi_{dB}^2}{2\sigma_{\psi_{dB}}^2} + \ln(10)\frac{\psi_{dB}}{10}\right) d\psi_{dB} \\ &= \beta \cdot d_n^{2\gamma}(\boldsymbol{\omega}) h_n^{-1} = \beta \cdot (h_n^{-1/\gamma} \|\mathbf{q}_n - \omega\|_2^2 + h_n^{2-1/\gamma})^{\gamma} \end{aligned} \tag{5}$$

defines then the nth *parameter distortion function* $D(\cdot, \mathbf{q}_n, h_n)$ with the independent

and fixed parameters

$$\beta = (2^{\frac{R_b}{B}} - 1)BN_0 \exp\big(-\frac{\sigma^2_{\psi_{dB}}(\ln 10)^2}{200}\big)(G_{\rm GT}K)^{-1}d_0^{-\alpha} \quad \text{and} \quad \gamma = \frac{\alpha+1}{2}. \tag{6}$$

For simplicity, we will set from here on $\beta = 1$, since it will not affect the quantizer.

3 Parameter Optimized Quantizers under Minimal Average Distortion

The communication power cost (5) defines therefore with $a_n = h_n^{-1/\gamma}$ and $b_n = h_n^{2-1/\gamma}$ for fixed $\gamma \geq 1$ a parameter dependent distortion function for $\mathbf{q}_n$. For a given source sample (GT) density λ in Ω and UAV deployment, the average power is the average distortion for given *parameter and quantization points* $(\mathbf{Q}, \mathbf{h})$ with quantization sets $\mathcal{R} = \{\mathcal{R}_n\}$, which is called the *average distortion* of the quantizer $(\mathbf{Q}, \mathbf{h}, \mathcal{R})$

$$\bar{D}(\mathbf{Q}, \mathbf{h}, \mathcal{R}) = \sum_{n=1}^{N} \int_{\mathcal{R}_n} D(\boldsymbol{\omega}, \mathbf{q}_n, h_n)\lambda(\boldsymbol{\omega})d\boldsymbol{\omega}. \tag{7}$$

The N quantization sets, which minimize the average distortion for given quantization and parameter points $(\mathbf{Q}, \mathbf{h})$, define a generalized Voronoi tessellation $\mathcal{V} = \{\mathcal{V}_n(\mathbf{Q}, \mathbf{h})\}$

$$\bar{D}(\mathbf{Q}, \mathbf{h}, \mathcal{V}) := \int_{\Omega} \min_n \{D(\boldsymbol{\omega}, \mathbf{q}_n, h_n)\}\, \lambda(\boldsymbol{\omega})d\boldsymbol{\omega} = \sum_n \int_{\mathcal{V}_n} D(\boldsymbol{\omega}, \mathbf{q}_n, h_n)\lambda(\boldsymbol{\omega})d\boldsymbol{\omega}, \tag{8}$$

where the *generalized Voronoi regions* $\mathcal{V}_n(\mathbf{Q}, \mathbf{h})$ are defined as the set of sample points $\boldsymbol{\omega}$ with smallest distortion (distance) to the nth quantization point $\mathbf{q}_n$ with parameter h_n. Minimizing the *average distortion* $\bar{D}(\mathbf{Q}, \mathbf{h}, \mathcal{V})$ over all parameter and quantization points defines an *$N-$facility locational-parameter optimization problem* [6]–[8], [21]. By the definition of the Voronoi regions (8) this is equivalent to the minimal average distortion over all $N-$level parameter quantizers

$$\bar{D}(\mathbf{Q}^*, \mathbf{h}^*, \mathcal{V}^*) = \min_{(\mathbf{Q},\mathbf{h})\in\Omega^N\times\mathbb{R}_+^N} \bar{D}(\mathbf{Q}, \mathbf{h}, \mathcal{V}) = \min_{(\mathbf{Q},\mathbf{h})\in\Omega^N\times\mathbb{R}_+^N} \min_{\mathcal{R}=\{\mathcal{R}_n\}\subset\Omega^N} \bar{D}(\mathbf{Q}, \mathbf{h}, \mathcal{R}). \tag{9}$$

which we call the *$N-$level parameter optimized quantizer*. To find local extrema of (8) analytically, we will need that the objective function $\bar{D}$ is continuously differentiable at any point in $\Omega^N \times \mathbb{R}_+^N$, i.e., the gradient exists and is a continuous function, as was shown for piecewise continuous non-decreasing distortion functions in the Euclidean metric over Ω^N [22, Thm.2.2] and [6]. We could extend this result in [23] to continuous distortion functionover arbitrary $d-$dimensional parameter sets in $\mathbb{R}^d$, which are analytical multivariate functions if restricted to Ω. Then the necessary condition for a local extrema is the vanishing of the gradient at a critical point. First we will derive the generalized Voronoi regions for convex sets Ω in d dimensions for any parameters $h_n \in \mathbb{R}_+$ for the quantization points $\mathbf{q}_n$, which are special cases of *Möbius diagrams*, introduced very recently in [4].

Lemma 1. *Let* $\mathbf{Q} = \{\mathbf{q}_1, \mathbf{q}_2, \dots, \mathbf{q}_N\} \subset \Omega^N \subset (\mathbb{R}^d)^N$ *for* $d \in \{1, 2\}$ *be the quantization points and* $\mathbf{h} = (h_1, \dots, h_N) \in \mathbb{R}_+^N$ *the associated parameters. Then the average distortion of* $(\mathbf{Q}, \mathbf{h})$ *over all samples in* Ω *distributed by* λ *for some exponent* $\gamma \geq 1$

$$\bar{D}(\mathbf{Q}, \mathbf{h}) = \sum_{n=1}^{N} \int_{\mathcal{V}_n} \frac{(\|\mathbf{q}_n - \boldsymbol{\omega}\|^2 + h_n^2)^\gamma}{h_n} \lambda(\boldsymbol{\omega}) d\boldsymbol{\omega} \tag{10}$$

has generalized Voronoi regions $\mathcal{V}_n = \mathcal{V}_n(\mathbf{Q}, \mathbf{h}) = \bigcap_{m \neq n} \mathcal{V}_{nm}$*, where the dominance regions of quantization point* n *over* m *are given by*

$$\mathcal{V}_{nm} = \Omega \cap \begin{cases} HS(\mathbf{q}_n, \mathbf{q}_m) & , h_m = h_n \\ B(\mathbf{c}_{nm}, r_{nm}) & , h_n < h_m \\ B^c(\mathbf{c}_{nm}, r_{nm}) & , h_n > h_m \end{cases} \tag{11}$$

with center and radii

$$\mathbf{c}_{nm} = \frac{\mathbf{q}_n - h_{nm}\mathbf{q}_m}{1 - h_{nm}} \quad \textit{and} \quad r_{nm} = \left(\frac{h_{nm}}{(1 - h_{nm})^2} \|\mathbf{q}_n - \mathbf{q}_m\|^2 + h_n^2 \frac{h_{nm}^{1-2\gamma} - 1}{1 - h_{nm}} \right)^{\frac{1}{2}}. \tag{12}$$

Here, we introduced the parameter ratio of the n*th and* m*th quantization point as*

$$h_{nm} = (h_m / h_n)^\gamma. \tag{13}$$

Example 1. We plotted in Figure 1 for $N = 2$ and $\Omega = [0, 1]^2$ the GT cells for a uniform distribution with UAVs placed on

$$\mathbf{q}_1 = (0.1, 0.2), h_1 = 0.5, \quad \text{and} \quad \mathbf{q}_2 = (0.6, 0.6), h_2 = 1 \tag{14}$$

If the second UAV reaches an altitude of $h_2 \geq 2.3$ its Voroni cell $\mathcal{V}_2 = \mathcal{V}_{2,1}$ will be empty and hence become "inactive".

3.1 Local optimality conditions

To find the optimal $N-$level parameter quantizer (8), we have to minimize the average distortion (7) over all possible parameter quantization points in $\mathcal{P}^N$, i.e., we have to solve a non-convex $N-$*facility locational-parameter optimization problem*,

$$\bar{D}(\mathbf{Q}^*, \mathbf{h}^*, \mathcal{V}^*) = \min_{\mathbf{Q} \in \Omega^N, \mathbf{h} \in \mathbb{R}_+^N} \sum_{n=1}^{N} \int_{\mathcal{V}_n(\mathbf{Q}, \mathbf{h})} h_n^{-1} (\|\mathbf{q}_n - \boldsymbol{\omega}\|^2 + h_n^2)^\gamma \lambda(\boldsymbol{\omega}) d\boldsymbol{\omega} \tag{15}$$

where $\mathcal{V}_n(\mathbf{Q}, \mathbf{h})$ are the Möbius regions given in (11) for each fixed $(\mathbf{Q}, \mathbf{h})$. A point $(\mathbf{Q}^*, \mathbf{h}^*)$ with Möbius regions $\mathcal{V}^* = \mathcal{V}(\mathbf{Q}^*, \mathbf{h}^*) = \{\mathcal{V}_1^*, \dots, \mathcal{V}_N^*\}$ is a critical point of

(15) if all partial derivatives of $\bar{D}$ are vanishing, i.e., if for each $n \in [N]$ it holds

$$0 = \int_{\mathcal{V}_n^*} (\mathbf{q}_n^* - \boldsymbol{\omega})(\|\mathbf{q}_n^* - \boldsymbol{\omega}\|^2 + h_n^{*2})^{\gamma-1} \lambda(\boldsymbol{\omega}) d\boldsymbol{\omega} \tag{16}$$

$$0 = \int_{\mathcal{V}_n^*} (\|\mathbf{q}_n^* - \boldsymbol{\omega}\|^2 + h_n^{*2})^{\gamma-1} \cdot (\|\mathbf{q}_n^* - \boldsymbol{\omega}\|^2 - (2\gamma-1)h_n^{*2}) \lambda(\boldsymbol{\omega}) d\boldsymbol{\omega} \tag{17}$$

For $N = 1$ the integral regions will not depend on $\mathbf{P}$ or $\mathbf{h}$ and since the integral kernel is continuous differentiable, the partial derivatives will only apply to the integral kernel. For $N > 1$ the conversation law of mass, can be used to show that the derivatives of the integral domains will cancel each other out, see also [23], [22].

3.2 The optimal $N-$level parameter quantizer in one-dimension for uniform density

In this section, we discuss the parameter optimized quantizer for a one-dimensional convex source $\Omega \subset \mathbb{R}$, i.e., for an interval $\Omega = [s, t]$. Under such circumstances, the quantization points are degenerated to scalars, i.e., $\mathbf{q}_n = x_n \in [s, t]$, $\forall\ n \in [N]$. If we shift the interval Ω by an arbitrary number $a \in \mathbb{R}$, then the average distortion, i.e., the objective function, will not change if we shift all quantization points by the same number a. Hence, if we set $a = -s$ we can shift any quantizer for $[s, t]$ to $[0, A]$ where $A = t - s$ without changing the average distortion. Let us assume a uniform distribution on Ω, i.e. $\lambda(\omega) = 1/A$. To derive the unique $N-$level parameter optimized quantizer we need first to derive the optimal $1-$level parameter quantizer.

Lemma 2. *Let $A > 0$ and $\gamma \geq 1$. The unique $1-$level parameter optimized quantizer (x^*, h^*) with distortion function (5), is given for a uniform source density in $[0, A]$ by*

$$x^* = \frac{A}{2}, \quad h^* = \frac{A}{2} g(\gamma) \quad \textit{and minimal average distortion} \quad \bar{D}(x^*, h^*) = \left(\frac{A}{2}\right)^{2\gamma-1} g(\gamma)$$

where $g(\gamma) = \arg\min_{u>0} F(u, \gamma) < 1/\sqrt{2\gamma - 1}$ is the unique minimizer of

$$F(u, \gamma) = \int_0^1 f(\omega, u, \gamma) d\omega \quad \textit{with} \quad f(\omega, u, \gamma) = \frac{(\omega^2 + u^2)^\gamma}{u} \tag{18}$$

which is for fixed γ a continuous and convex function over $\mathbb{R}_+$. The global minimum can be derived in closed form for integer valued γ as

$$g(1) = \sqrt{1/3}, \quad g(2) = \sqrt{(\sqrt{32/5} - 1)/9}, \quad g(3) = \sqrt{\left((32/7)^{1/3} - 1\right)/5}. \tag{19}$$

Remark. The convexity of $F(\cdot, \gamma)$ can be also shown by using extensions of the Hermite-Hadamard inequality [24], which allows to show convexity over any interval. This suggest, that as long as the generalized Voronoi regions remain convex, the objective function might be still convex. Let us note here, that for any fixed parameter $h_n > 0$, the average distortion $\bar{D}(x_n^* \pm \epsilon, h_n)$ is strictly monotone increasing in $\epsilon > 0$.

Hence, x_n^* is the unique minimizer for any $h_n > 0$. We will use this decoupling property repeatedly in the proofs.

To derive our main result, we need some general properties of the optimal regions.

Lemma 3. *Let $\Omega = [0, A]$ for some $A > 0$. The $N-$level parameter optimized quantizer $(\mathbf{Q}^*, \mathbf{h}^*) \in \Omega^N \times \mathbb{R}_+^N$ for a uniform source density in Ω has optimal quantization regions $\mathcal{V}_n(\mathbf{Q}^*, \mathbf{h}^*) = [b_{n-1}^*, b_n^*]$ with $0 \leq b_{n-1}^* < b_n^* \leq A$ and optimal quantization points $x_n^* = (b_n^* + b_{n-1})/2$ for $n \in [N]$, i.e., each region is a closed interval with positive measure and centroidal quantization points.*

Remark. Hence, for an $N-$level parameter optimized quantizer, all quantization points are used, which is intuitively, since each quantization point should reduce the distortion of the quantizer by partitioning the source in non-zero regions.

Theorem 1. *Let $N \in \mathbb{N}$, $\Omega = [0, A]$ for some $A > 0$, and $\gamma \geq 1$. The* unique *$N-$*level parameter optimized quantizer *$(\mathbf{Q}^*, \mathbf{h}^*, \mathcal{R}^*)$ is the uniform scalar quantizer with identical parameter values, given for $n \in [N]$ by*

$$\mathbf{q}_n^* = x_n^* = \frac{A}{2N}(2n-1), \quad h^* = h_n^* = \frac{A}{2N} g(\gamma), \quad \mathcal{R}_n^* = \left[\frac{A}{N}(n-1), \frac{A}{N} n\right] \tag{20}$$

with minimal average distortion

$$\bar{D}(\mathbf{Q}^*, \mathbf{h}^*, \mathcal{R}^*) = \left(\frac{A}{2N}\right)^{2\gamma-1} \int_0^1 \frac{\left(\omega^2 + g^2(\gamma)\right)^\gamma}{g(\gamma)} d\omega. \tag{21}$$

For $\gamma \in \{1, 2, 3\}$ we can derive $g(\gamma)$ in closed form (19).

Example 2. We plotted in Figure 2 the optimal heights and optimal average distortion for a uniform GT density in $[0, 1]$ over various α and $N = 2$. Note, that the factor $A/2N = 1/4$ will play a crucial role for the height and distortion scaling. Moreover, the distortion decreases exponentially in α if $A/2N < 1$.

Let us set $\beta = 1 = A$. Then the optimal UAV deployment is pictured in Figure 3 for $N = 2$ and $N = 4$. The maximal evaluation angle $\theta_{\max}$ is hereby constant for each UAV and does not change if the number of UAVs N increase. Moreover, it is also independent of A and β, since with (20) we have $d_n = x_n^* - x_{n-1}^* = A/N$ and

$$\cos(\theta_{\max}) = \cos(\theta_n) = \frac{h^*}{d_n^*/2} = \frac{2N}{A} \frac{A}{2N} g(1) = \frac{1}{\sqrt{3}}. \tag{22}$$

4 Numerical Algorithms and Simulation Results over Two-Dimensions

In this section, we introduce two Lloyd-like algorithms, Lloyd-A and Lloyd-B, to optimize the quantizer. The proposed algorithms iterate between two steps: (1) The

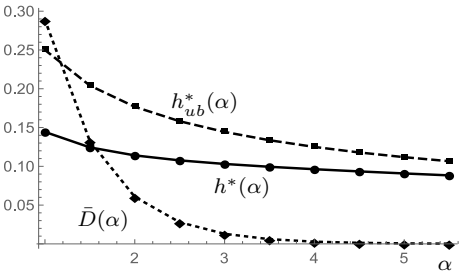

Figure 2: Optimal height (solid) with bound (dashed) and average distortion (dotted) for $N = 2, A = 1$ and uniform GT density.

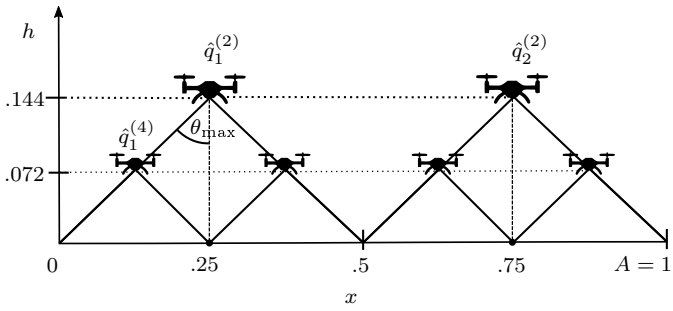

Figure 3: Optimal UAV deployment in one dimension for $A = 1, \alpha = 1$ and $N = 2, 4$ over a uniform GT density by (20).

reproduction points are optimized through gradient descent while the partitioning is fixed; (ii) The partitioning is optimized while the reproduction points are fixed. In Lloyd-A, all UAVs (or reproduction points) share the common flight height while Lloyd-B allows UAVs to flight on different heights.

In what follows, we provide the simulation results over the two-dimension target region $\Omega = [0, 10] \times [0, 10]$ with uniform and non-uniform density functions. The non-uniform density function is a Gaussian mixture of the form $\sum_{k=1}^{3} \frac{A_k}{\sqrt{2\pi\sigma_k^2}} \exp\left(-\frac{\|\omega - c_k\|^2}{2\sigma_k}\right)$, where the weights, A_k, are 0.5, 0.25, 0.25, the mean, c_k, are $(3, 3)$, $(6, 7)$, $(7.5, 2.5)$, the standard deviations, σ_k, are 1.5, 1, and 2.

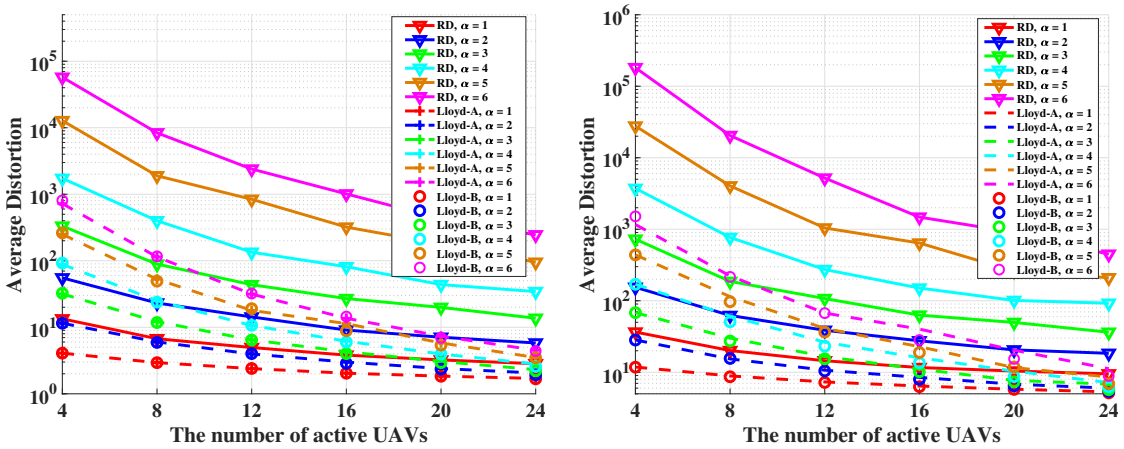

(a) (b)

Figure 4: The performance comparison of Lloyd-A, Lloyd-B and Random Deployment (RD). (a) Uniform density. (b) Non-uniform density.

To evaluate the performance of the proposed algorithms, we compare them with the average distortion of 100 random deployments (RD). Figs. 4a and 4b, show that the proposed algorithms outperform the random deployment on both uniform and non-uniform distributed target region. From 4a, one can also find that the distortion achieved by Lloyd-A and Loyd-B are very close, indicating that the common height property in one-dimension region might be extended to two-dimension region when

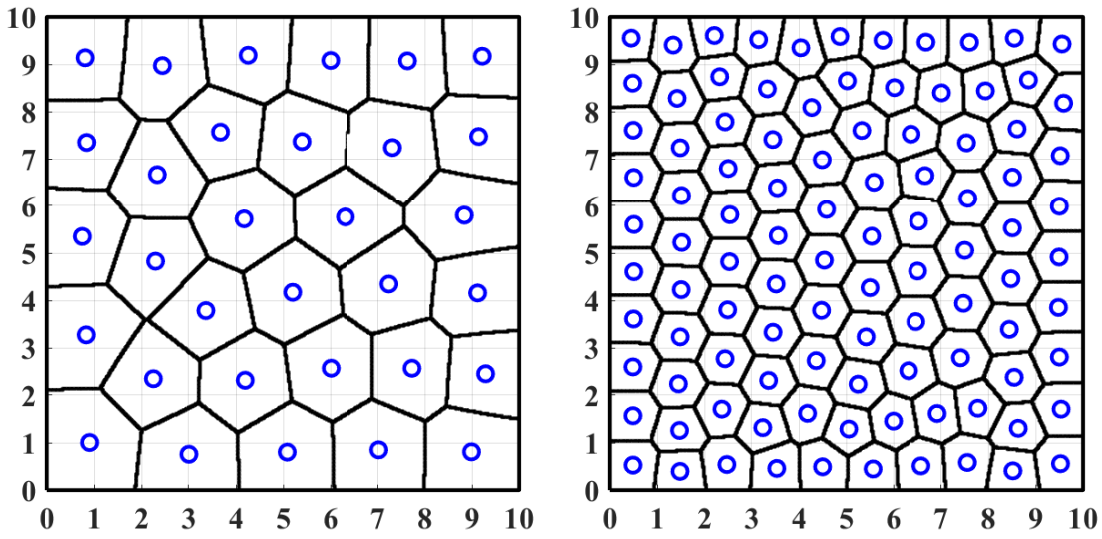

(a) (b)

Figure 5: The UAV projections on the ground with generalized Voronoi Diagrams where $\alpha = 2$. (a) 32 UAVs. (b) 100 UAVs.

the density function is uniform. However, one can find an nonnegligible gap between Lloyd-A and Lloyd-B from Fig. 4b where the density function is non-uniform. For instance, given 16 UAVs and pass loss exponent $\alpha = 6$, Lloyd-A's distortion is 40.17 while Lloyd-B obtains a smaller one, 28.25, by placing UAVs on different heights. Figs. 5a and 5b illustrate the UAV ground projections and their partitions on a uniform distributed region. As the number of UAVs increases, the UAV partitions approximate to be hexagons which implies the common height property (Theorem 1) might be extended to uniform distributed two-dimension. However, our simulations in [5] show that the common height is no longer a necessary condition for the optimal quantizer when distribution is non-uniform.

5 Conclusion

A new parameter weighted quantizer and its applications are studied in this paper. Instead of using the traditional mean distance square as the distortion, we introduce a distortion function which models the energy consumption of UAVs in dependence of their heights. We derived the unique parameter optimized quantizer - a uniform scalar quantizer with an optimal common weight - for uniform source density in one-dimensional space. In addition, two Lloyd-like algorithms are designed to minimize the distortion in two-dimensional space. Numerical simulations demonstrate that for a uniform density the common weight property extends to two-dimensional space.

[1] E. Koyuncu and H. Jafarkhani, "On the minimum distortion of quantizers with heterogeneous reproduction points," *DCC*, 2016.

[2] ——, "On the minimum average distortion of quantizers with index-dependent distortion measures," *IEEE Trans. Signal Process.*, vol. 65, no. 17, pp. 4655–4669, 2017.

[3] E. Koyuncu, R. Khodabakhsh, N. Surya, and H. Seferoglu, "Deployment and trajectory optimization for UAVs: A quantization theory approach," in *2018 IEEE Wireless Communications and Networking Conference (WCNC)*, IEEE, 2018. eprint: 1708.08832v5.

[4] J.-D. Boissonnat, C. Wormser, and M. Yvinec, "Curved voronoi diagrams," in *Effective Computational Geometry for Curves and Surfaces*. Springer, 2007, pp. 67–116.

[5] J. Guo, P. Walk, and H. Jafarkhani, "On the minimal average distortion of parameter optimized quantizers," *arxiv*, 2018.

[6] J. Guo and H. Jafarkhani, "Sensor deployment with limited communication range in homogeneous and heterogeneous wireless sensor networks," *IEEE Transactions on Wireless Communications*, vol. 15, no. 10, pp. 6771–6784, 2016.

[7] J. Guo, H. Jafarkhani, and E. Koyuncu, "A source coding perspective on node deployment in two-tier networks," *IEEE Trans. Commun.*, vol. 66, no. 7, pp. 3035–3049, 2018.

[8] J. Guo and H. Jafarkhani, "Movement-efficient sensor deployment in wireless sensor networks," *ICC*, 2018. arXiv: 1710.04746.

[9] M. Moarref and L. Rodrigues, "An optimal control approach to decentralized energy-efficient coverage problems," 3, vol. 47, Elsevier BV, 2014, pp. 6038–6043.

[10] M. T. Nguyen, L. Rodrigues, C. S. Maniu, and S. Olaru, "Discretized optimal control approach for dynamic multi-agent decentralized coverage," in *ISIC*, 2016.

[11] B. Galkin, J. Kibilda, and L. A. DaSilva, "Backhaul for low-altitude uavs in urban environments," in *ICC*, 2018.

[12] M. M. Azari, F. Rosas, and S. Pollin, "Reshaping cellular networks for the sky: Major factors and feasibility," *arxiv*, 2017.

[13] H. Shakhatreh and A. Khreishah, "Maximizing indoor wireless coverage using uavs equipped with directional antennas," *arxiv*, 2017.

[14] K. Venugopal, M. C. Valenti, and R. W. Heath, "Device-to-device millimeter wave communications: Interference, coverage, rate, and finite topologies," *IEEE Transactions on Wireless Communications*, vol. 15, no. 9, pp. 6175–6188, 2016.

[15] H. He, S. Zhang, Y. Zeng, and R. Zhang, "Joint altitude and beamwidth optimization for uav-enabled multiuser communications," *IEEE Communication Letters*, vol. 22, no. 2, 2018.

[16] M. Mozaffari, W. Saad, M. Bennis, and M. Debbah, "Efficient deployment of multiple unmanned aerial vehicles for optimal wireless coverage," *IEEE Communications Letters*, vol. 20, no. 8, pp. 1647–1650, 2016.

[17] A. Goldsmith, *Wireless communications*. Cambridge University Press, 2005.

[18] M. Mozaffari, W. Saad, M. Bennis, and M. Debbah, "Unmanned aerial vehicle with underlaid device-to-device communications: Performance and tradeoffs," *IEEE Transactions on Wireless Communications*, vol. 15, no. 6, pp. 3949–3963, 2016.

[19] A. Al-Hourani and K. Gomez, "Modeling cellular-to-UAV path-loss for suburban environments," *IEEE Wireless Communications Letters*, vol. 7, no. 1, pp. 82–85, 2018.

[20] C. A. Balanis, *Antenna theory: Analysis and design*. Wiley-Interscience, 2005, p. 1136.

[21] A. Okabe, B. Boots, K. Sugihara, and S. N. Chiu, *Spatial tessellations: Concepts and applications of voronoi diagrams*, 2nd. John Wiley & Sons, 2000.

[22] J. Cortés, S. Martínez, and F. Bullo, "Spatially-distributed coverage optimization and control with limited-range interactions," *ESAIM*, vol. 11, no. 4, pp. 691–719, 2005.

[23] P. Walk and H. Jafarkhani, "Continuous locational-parameter optimization problems," *in preparation*, 2018.

[24] X. M. Zhang and Y. M. Chu, "Convexity of the integral arithmetic mean of a convex function," *Rocky Mountain Journal of Mathematics*, vol. 40, no. 3, pp. 1061–1068, 2010.